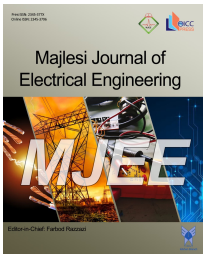

Volume 19, Issue 2, 192539 (1-13)

Majlesi Journal of Electrical Engineering (MJEE)

https://doi.org/10.57647/j.mjee.2025.6p89

Adaptive reversible data hiding scheme based on novel cascading prediction error histogram shifting using decimal floating stream

Reza Ghorbandost Soveiri[1,*], Maryam Rajabzadeh Asaar[1], Pouya Derakhshan Barjoei[2]

[1]*Cyber Security Research Center, Department of Electrical Engineering, SR.C, Islamic Azad University, Tehran, Iran.*
[2]*Artificial Intelligence and Data Analysis Research Center, Department of Electrical Engineering, SR.C., Islamic Azad University, Tehran, Iran.*

[*]**Corresponding author:** reza.ghorbandost@srbiau.ac.ir

Original Research

Received:
4 December 2024
Revised:
27 February 2025
Accepted:
14 March 2025
Published online:
1 June 2025

Abstract:

Today, with the development of processing technologies and improvement in cloud networks, a large number of photos are transferred in networks. The need to hide data and maintain security attracted the attention of researchers. In this paper, a reversible data hiding method based on the prediction error histogram shifting is proposed in order to increase the embedding capacity and maintains the visual quality of the image as well. To reach these goals, the original image is transformed into block-wise and for each block the prediction method is figured based on the proposed method to create prediction errors. According to our prediction method, in each 4×4 block, 75% of the prediction error pixels can find the ability to embed information. The experimental results show a good acceptable embedding capacity as it is clear in a sample test image of an airplane. In this case, the embedding capacity of 206,270 bits and a Peak Signal-to-Noise Ratio (PSNR) of 50.99 dB have been reached. These results show the efficiency of our proposed method based on the embedding capacity and visual quality of the images. The outcomes of the proposed method reach better results than the main competitor methods.

Keywords: Reversible data hiding; Histogram shifting; Prediction error; Embedding capacity; Visual quality

1. Introduction

Data hiding refers to embedding the information and data as a binary stream in digital multimedia such as image, audio and video. In fact, data hiding is the undetectable change of a work to embed a message.

This embedding has no obvious and visible change in multimedia and all information embedded in multimedia is well extracted by its receiver. Today, due to the need for easy transfer and movement of important and confidential information like military, medical, authentication or other fields from one place to another, this technology has been receiving attention and welcomes day by day.

Considering the digital images, there are various methods of data hiding in the spatial domain, such as LSB [1–11], DE [12–18], HS [19–30], Interpolation [31–35], so that the information is embedded in the place of the pixels according to it. In general, data hiding in images is divided into two categories. These categories are taken into account as reversible data hiding and irreversible data hiding. In a reversible data hiding scheme, the embedded information is well extracted and also the stego image is recovered in its original form. In the irreversible data hiding scheme, despite the information extraction, the method is not capable of recovering the stego image in its original form.

Among the data hiding methods in the spatial domain, Difference Expansion (DE) and Histogram Shifting (HS) are two very common and important methods in reversible data hiding schemes, which have the ability to embed a large amount of information. Schemes based on HS histogram shifting [19–30] have attracted the attention of most researchers. In 2006 Ni et al. [19] for the first time, proposed a reversible data hiding scheme based on histogram shifting. In this method, the histogram of the cover image is created at first, then one or more pairs of peak and zero points are

selected according to the requirement of Embedding Capacity (EC); Then, the pixels between the peak and zero points are shifted by one unit in the direction of the zero point to free up space for data embedding. In the next step, the information is embedded in the pixels with the maximum size in the histogram. The size of the embedding capacity is determined by the maximum size in the histogram of the cover image. The stego image has good quality because the maximum change of pixels is one in a unit ($\Delta = 1$).

In order to achieve a higher embedding capacity, much research was conducted for the HS-based design and some ideas were proposed. Some divided the cover image into two parts and applied the HS method separately for each part [20]. Also, others used multi-layer and multi-level embedding in the image histogram [25, 27], however, there are methods that used the prediction-error histogram shift method as developed in recent years [21–24, 26, 30]. First, the original image, the cover image, is processed using prediction methods, then the prediction error of the image is calculated. After that, the information is embedded in the prediction error instead of the original image. One of the ways to improve the embedding capacity is to use a more advanced prediction method to obtain a histogram with a relatively clearer density distribution. The motivation of the research in the literature focused on the hiding of data and information in general. Our contribution to this research is to implement a reversible data hiding method based on the prediction-error histogram shifting. In this research, also, we proposed an adaptive method in order to increase the embedding capacity. Besides that, maintaining the visual quality of the image is considered as well.

2. Related works

With a simple search about data hiding and steganography, we may find much good research in this area, in different schemes. Information and data hiding performance in images is an interesting topic for researchers. Here we mentioned some related research about that, however, we can find more different aspects of view in this area. In 2009 Tsai et al. [23] used the linear prediction technique and achieved a significant embedding capacity. In 2015 Hu et al. [26] proposed a method based on cascade prediction and improved the embedding capacity. First, they divided the original image into 4×4 or 5×5 blocks and embedded the information in the prediction error based on their prediction model. In 2020, Xie et al. [30] investigated the method of Hu et al. [26]. They considered signed-digit as embeddable data. they represented and converted the binary stream into a signed-digit stream. They first reduced the number of binary digit "1" in the binary stream, so that the changes of the prediction error after embedding the information are minimized and the image distortion is reduced. Finally, the image quality is improved. In their method, several peak points in the prediction error histogram were considered and the cover image was divided into 2×2 or 4×4 or 8×8 blocks and the prediction error was calculated using cascade prediction.

In the method that is presented by Xie et al., the embedding capacity was matched with the dimensions of the block [30]. In [30], Xie et al. investigated that the image quality decreases with increasing embedding capacity. Therefore, in the mentioned method, there should be a balance between embedding capacity and image quality. Also, the embedding capacity is affected by the number of selected peaks points. According to the results of the tests, increasing the maximum number of points n, increases the embedding capacity and consequently increases the distortion of the image and reduces the quality of the cover image. These results are the same for all image block-wise dimensions. Of course, according to the results of the above method, it works better for the block with dimensions of 4×4. In the method of Xie et al. [30], the image embedding capacity has been significantly increased at the cost of reducing the image quality under factors such as the maximum number of points n and the dimensions of the image block. Among other features of this method, we can mention the arbitrary selection of the maximum number of points n for data embedding and achieving adaptive embedding capacity. The remaining parts of the paper are organized as follows. Our proposed scheme is presented in section 3. Experimental results are given in section 4, with some concluding remarks and future work suggestions in section 5.

3. Proposed scheme

According to the investigated research and method by Hu et al. [26] and Xie et al. [30], we define our proposed scheme. Fig. 1 shows the framework of our proposed scheme.

Based on these studies our proposed scheme is explained

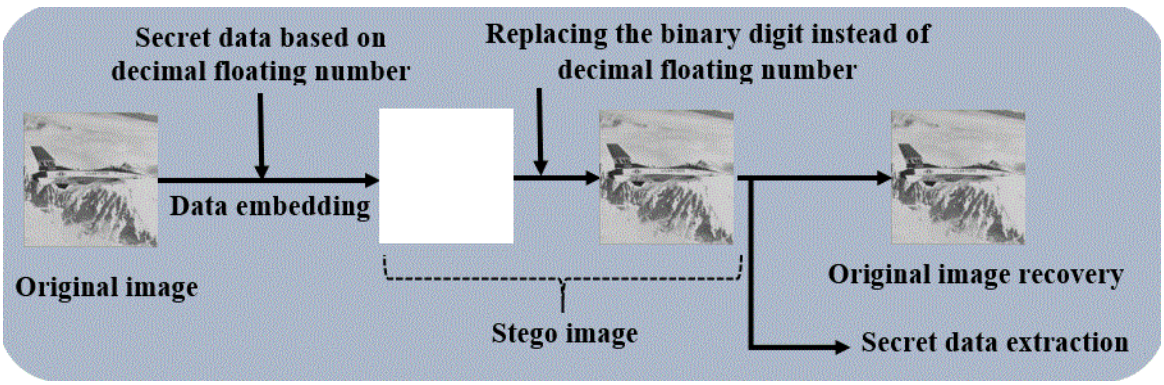

Figure 1. The framework of our proposed scheme.

as follow. At first, we divided the original image, the cover image, into 4×4 blocks as shown in Fig. 2 (a). Selecting the reference pixel for all 4×4 blocks of original image, the prediction is made based on the proposed scheme based on Fig. 2 (b) and then the prediction error is calculated as shown in Fig. 2 (c). As seen in Fig. 2, in each 4×4 block of the original image, $3/4$ of the prediction error becomes zero, and as a result, the peak of the histogram of the prediction error image is determined at point "0", that is, a place for embedding information. In this method, we used a pair of peak and zero points to perform the histogram shifting operation and then embed the information, which helps to increase the visual quality of the image and reduce the distortion of the image as much as possible. Our proposed method there are two properties, the simplicity of its algorithm due to having only one pair of maximum and zero points and using the conversion of binary data stream "S" with one conversion step to decimal floating data stream, and replacing allocated binary digit instead of decimal floating number to creating the main stego image in the encoder and decoder.

3.1 Block–wise prediction based on the proposed scheme

Fig. 2 illustrates that in the first step, we divided the original image into 4×4 blocks. In each 4×4 block, we select the pixel P_{33} as the reference pixel, and by replacing it with P_{22}, P_{24}, P_{42}, and P_{44}, we obtain the prediction matrix of the proposed method in this paper as shown in Fig. 2 (b). Finally, the difference of the original image is taken from the prediction matrix, which leads to the prediction error of the original image. The important point is that according to the characteristics of the prediction function in the our method, in each 4×4 block of the image, 75% of each block finds the ability to data embedding, see Fig. 2.
Fig. 3 shows the comparison of the histogram of the original image and the histogram of the original image prediction error. As it is clear in the Figure, the peak amplitude of the histogram in the original image prediction error has increased significantly compared to the peak amplitude of the histogram of the original image.

$$d = P_x - P_r \tag{1}$$

$$d_{\text{new}} = \begin{cases} d+1, & \text{if } d \geq 1 \\ d, & \text{otherwise.} \end{cases} \tag{2}$$

3.2 Information embedding procedure

Fig. 4 shows the block diagram of the information embedding procedure based on the proposed method, and these steps are described as follow:
Input: Original image (P_x) and main secret data "S".
Output: Marked image (P_{xnew}).
Step 1: Calculation of the prediction function based on the proposed method (P_r), see Fig. 2 (b) and Fig. 8.

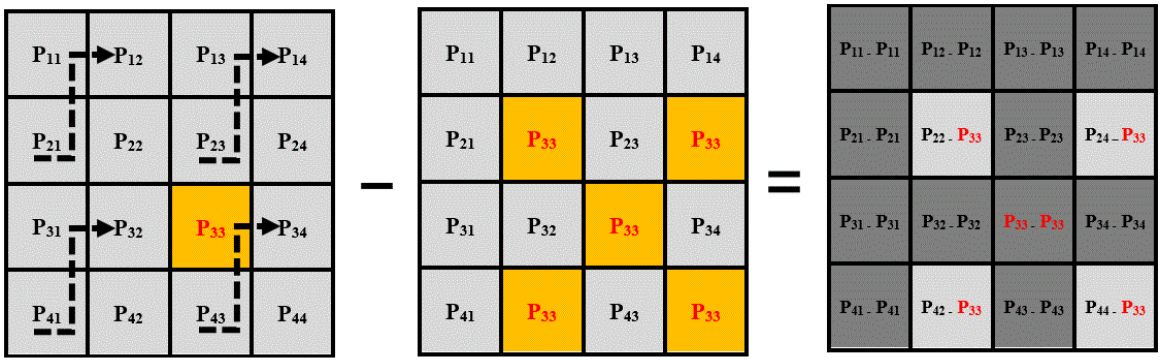

(a) Original image (b) Proposed prediction (P_r) (c) Prediction error (d)

Figure 2. Proposed scheme for 4×4 block-wise prediction.

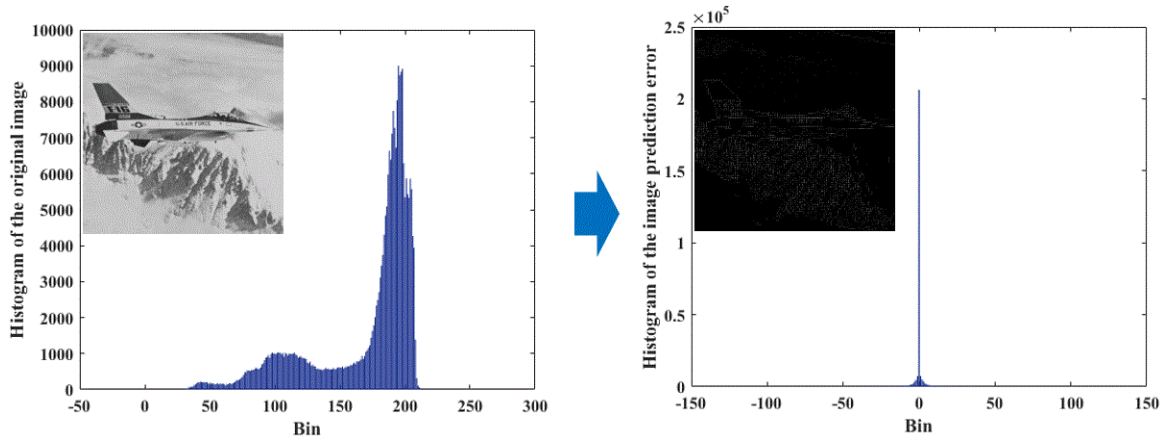

Figure 3. Histogram of the original image and the prediction error.

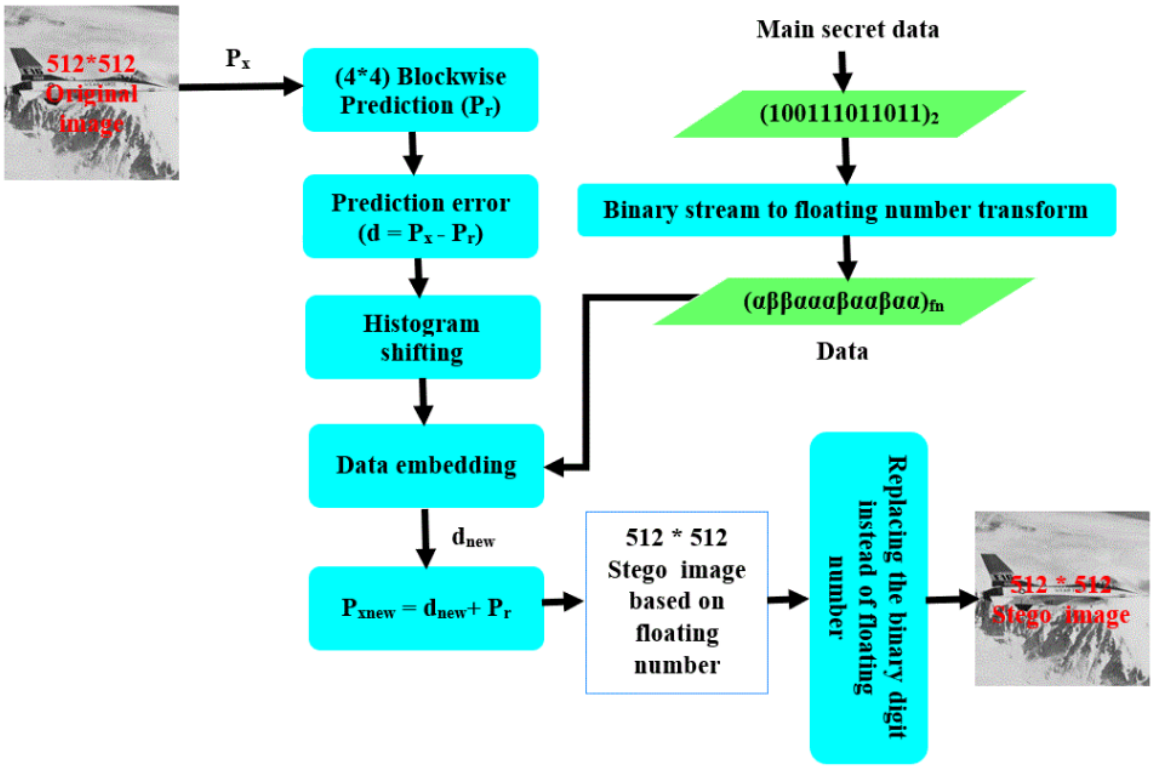

Figure 4. Information embedding procedure based on the proposed method.

Step 2: Calculation of prediction error according to Eq. (1) and Fig. 2 (c).
Step 3: Taking the histogram of the image prediction error (d), shifting the histogram based on the selection of a pair of maximum and zero points according to Eq. (2).
Step 4: Conversion of binary data stream "S" with one conversion steps to decimal floating data stream according to Eq. (3).
Step 5: Embedding the data in the maximum point of the shifted prediction error histogram (d_{new}) according to Eq. (4).
Step 6: Combining the prediction function of the original image with the embedded prediction error (d_{new}), we create the stego image based on floating number in the output according to Eq. (5).
Step7: Replacing binary digit instead of decimal floating number and finally creating the stego image (P_{xnew}), see Eq. (6).

$$(\text{data})_2 \text{ to } (\text{data})_{\text{fn}} = \begin{cases} 0 < \beta < B, & \text{if } S_i = 0 \\ C < \alpha < 1, & \text{if } S_i = 1. \end{cases} \tag{3}$$

$$d_{\text{new}} = \begin{cases} d_{\text{new}} + S, & \text{if } d_{\text{new}} = 0 \\ d_{\text{new}}, & \text{otherwise.} \end{cases} \tag{4}$$

$$\text{P}_{\text{xnew}} = d_{\text{new}} + \text{P}_r \tag{5}$$

$$(\text{data})_{\text{fn}} \text{ to } (\text{data})_2 = \begin{cases} S_i = 0, & \text{if } 0 < \beta < B \\ S_i = 1, & \text{if } C < \alpha < 1. \end{cases} \tag{6}$$

3.3 Information extraction and original image recovery procedure

The block diagram of the information extraction and original image recovery procedure based on the proposed method is shown in Fig. 5. These steps are described as follow:
Input: Marked image based on decimal floating number stream.
Output: Recovered original image (P_x) and extracted main secret data "S".
Step 1: Receiving the stego image based on decimal floating number and then replacing the binary digits instead of decimal floating number (Eq. (6)) and Creating the stego image based on binary digits.
Step 2: Recovery of the prediction function of the proposed method (P_r) using stego image based on decimal floating number according to Fig. 8.
Step 3: Calculate the modified prediction error (d_{new}) of the stego image according to Eq. (7).
Step 4: Extract information (S) from the modified prediction error (d_{new}) of the stego image according to Eq. (8).
Step 5: In the end of taking the prediction error histogram of the stego image, recovery of the prediction error of the original image according to Eq. (9) and reverse shifting according to Eq. (10) and combine it with the prediction function of the original image according to Eq. (11).

$$d_{\text{new}} = \text{P}_{\text{xnew}} - \text{P}_r \tag{7}$$

$$S = \begin{cases} 1, & \text{if } d_{\text{new}} = 1 \\ 0 & \text{if } d_{\text{new}} = 0. \end{cases} \tag{8}$$

$$d_{\text{new}} = \begin{cases} 0, & \text{if } d_{\text{new}} = 1 \\ d_{\text{new}} & \text{otherwise.} \end{cases} \tag{9}$$

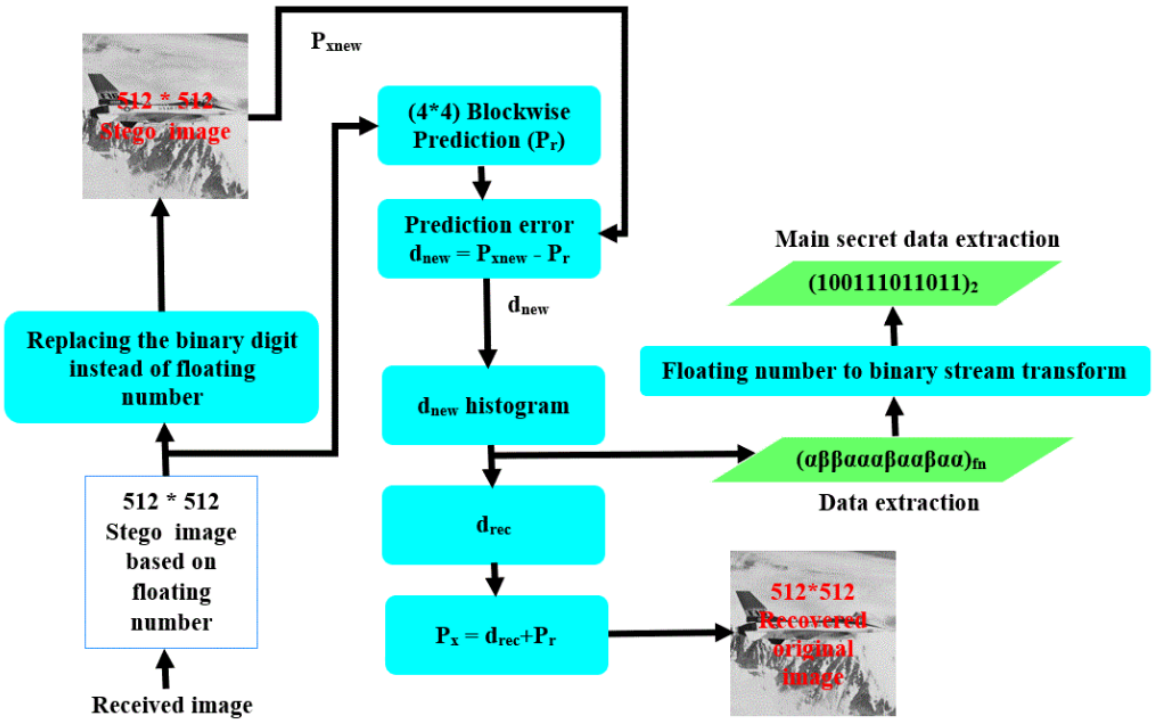

Figure 5. Information extraction and original image recovery procedure based on the proposed method.

$$d_{\text{rec}} = \begin{cases} d_{\text{new}} - 1, & \text{if } d_{\text{new}} \geq 1 \\ d_{\text{new}} & \text{otherwise.} \end{cases} \tag{10}$$

$$\mathrm{P}_x = d_{\text{rec}} - \mathrm{P}_r \tag{11}$$

3.4 Example of the proposed scheme

For better understanding an example is given in this section in order to verify the procedure. Fig. 6 shows the process of information embedding in the transmitter and Fig. 7 shows the process of information extraction and original image recovery in the receiver.

First, the original image is divided into 4×4 blocks. For each block, the embedding process is similar to the example in Fig. 6. Based on our proposed prediction method, the prediction error is calculated. Then the shift operation of the histogram of the prediction error is performed in the range of the maximum and zero points of the prediction error histogram. In the next step information of the binary stream $(\alpha\beta\beta\alpha\alpha\alpha\beta\alpha\alpha\beta\alpha\alpha)_{\text{fn}}$ is embedded in it. Finally, by combining the prediction function of the original image will obtain the stego image. In Fig. 7, the example of the process of information extraction and original image recovery are shown. The marked image is received as a 4×4 block, then based on the prediction function of our proposed method, the prediction error calculated, in the first step of the binary stream information $(100111011011)_2$ is correctly extracted, in the following, the prediction error recovery steps are followed and original image is recovered.

3.5 Example of prediction function recovery and achieve to original marked image

We applying the secret data to recover the prediction function and achievement the original marked image in the receiver. In the binary stream $(100111011011)_2$ instead of the number 1, we temporarily use floating numbers in the range of $0.5 < \alpha < 1$ and instead of the number 0, floating numbers in the range of $0 < \beta < 0.5$ is used. Which leads to the corresponding data as: $(0.9141\ 0.2379\ 0.1613\ 0.8480\ 0.8068\ 0.8240\ 0.1637\ 0.9964\ 0.9530\ 0.3358\ 0.9276\ 0.8182)_{\text{fn}}$. After embedding this data, the changes of the embedded pixels are displayed as a decimal. Then, in the receiver, we proceed the following procedure and based on Fig. 8 to reach the main specified image and restore the prediction function.

Input: Input image (Ix).
Output 1: Original marked image recovery (P_{xnew}).
Output 2: Prediction function recovery (P_r).
Step 1: Round the input image matrix to the largest integer or smallest integer and convert it to the original marked image by the formula (P_{xnew} = round (Ix)).
Step 2: Round the input image matrix to the smallest integer by the formula (P_r = floor (Ix)) and then replace pixel P_{33} instead of the pixels P_{22}, P_{24}, P_{42}, and P_{44}. Also in the prediction function (P_r) size of pixel P_{33} is remains constant.

4. Experimental results

In order to check the steps of the algorithm experimentally, we applied standard and custom images. These 6 standard images are Airplane, Boat, Girl, Goldhill, Lena and Toy. These images are in gray scale with size of 512×512 [36, 37], as shown in Fig. 9, in order to measure and compare the results of the algorithm with other previous mentioned method, several important measurement criteria MSE, PSNR, SSIM and ER were used [38]. The Embedding Rate (ER) was used to measure the data

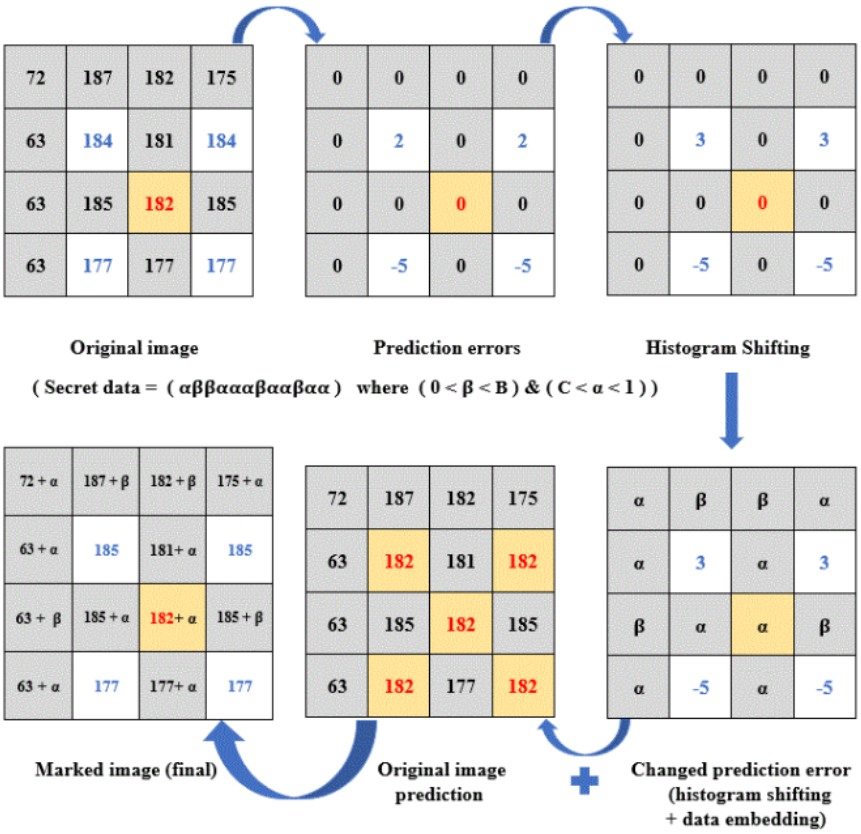

Figure 6. Information embedding process in the transmitter.

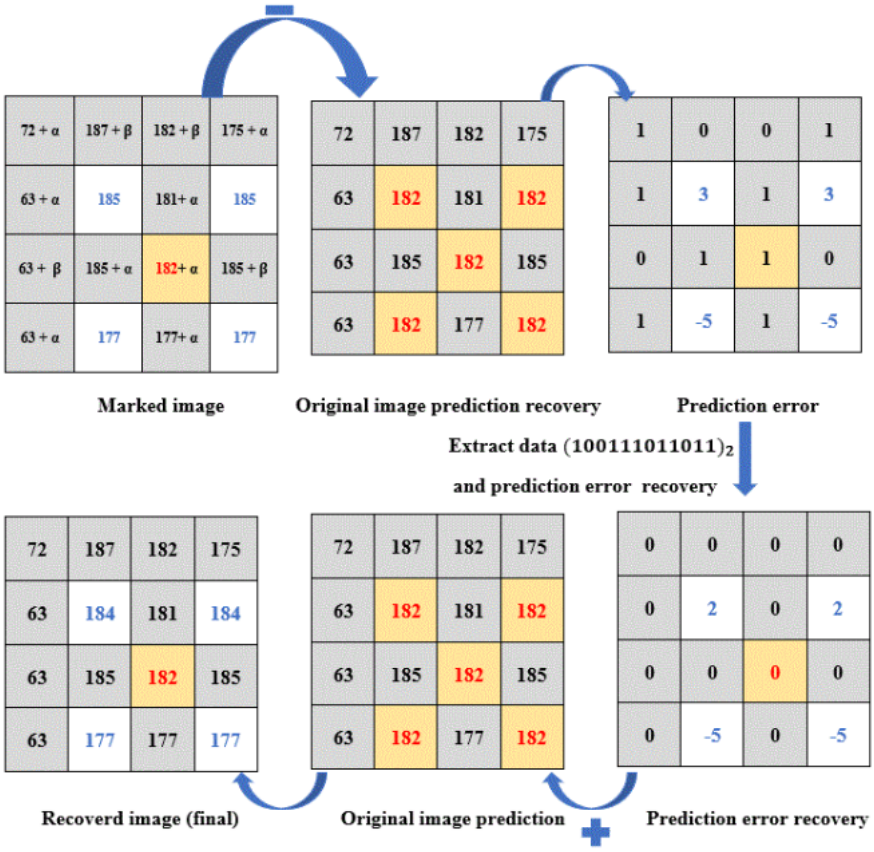

Figure 7. Information extraction and original image recovery process in the receiver.

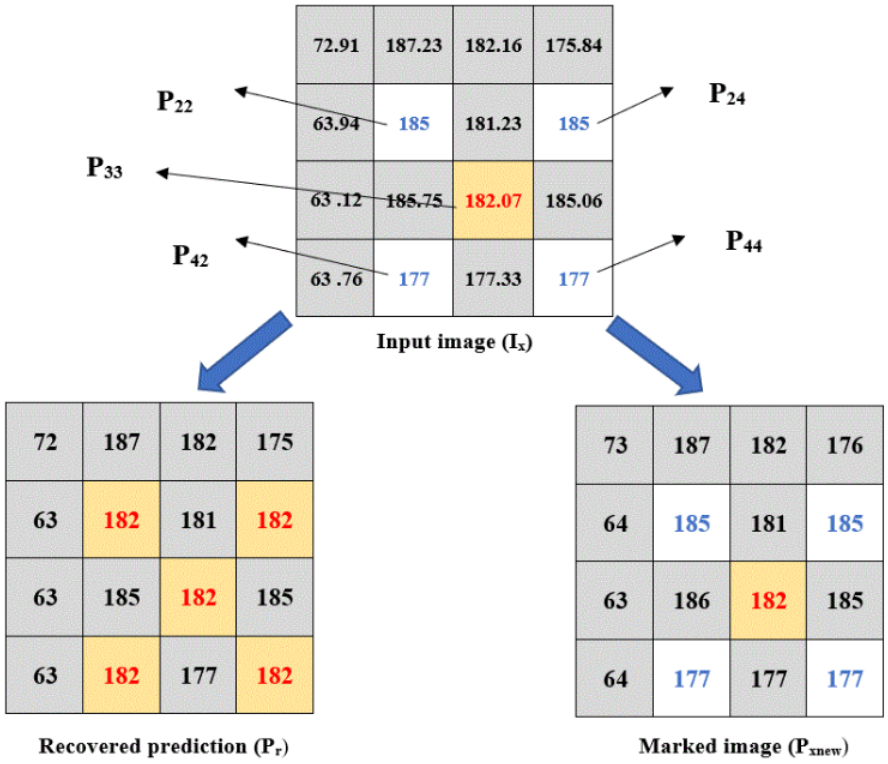

Figure 8. The method for achievement of original marked image and prediction function recovery.

hiding efficiency by Eq. (12).

$$\mathrm{ER} = \frac{\text{Number of sedret data}}{\text{Image size}}(\text{bpp}) \tag{12}$$

The bpp refers to bits per pixel. The higher embedding rate shows that this method can embed a large amount of secret information in the cover image. Also, maximum peak signal-to-noise ratio (PSNR) is used to measure the similarity between the original image and the marked image, using Eq. (13).

A higher PSNR value indicates that the marked image is very similar to the original image, therefore, the human eye cannot identify effectively the difference between the stego image and the original image.

$$\mathrm{PSNR} = 10 \times \log_{10} \frac{(255)^2}{\mathrm{MSE}}(\text{db}) \tag{13}$$

The MSE shows the mean square error between the original image and the stego image, the Eq. (14) shows it. Where, in this equation $(H \times W)$ refers to the image size.

$$\mathrm{MSE} = \frac{1}{H \times W} \times \sum_{i=1}^{H} \sum_{j=1}^{W} (\mathrm{P}(i,j) - \acute{\mathrm{P}}(i,j))^2 \tag{14}$$

In addition, the Structural Similarity index (SSIM) is calculated to measure the visual similarity between the cover image and the stego image as shown in Eq. (15).

$$\mathrm{SSIM}(\mathrm{P},\acute{\mathrm{P}}) = [l(\mathrm{P},\acute{\mathrm{P}})]^{\alpha} \times [c(\mathrm{P},\acute{\mathrm{P}})]^{\beta} \times [S(\mathrm{P},\acute{\mathrm{P}})]^{\gamma} \ \alpha,\beta,\gamma = 1 \tag{15}$$

Larger values of SSIM assure that the human eye system cannot effectively detect secret data from the stego image.

In this equation, P and $\acute{\mathrm{P}}$ denote the cover image and the stego image, respectively. The three parameters l, c and S show luminance contrast and structure, respectively. The value of luminance was calculated by Eq. (16):

$$l(\mathrm{P},\acute{\mathrm{P}}) = \frac{2 \times \overline{\mathrm{P}} \times \overline{\mathrm{P}}' + c}{\overline{\mathrm{P}}^2 \times (\overline{\mathrm{P}}')^2 + c} \tag{16}$$

where $\overline{\mathrm{P}}$ and $\overline{\mathrm{P}}'$ denote the average values of the cover pixels and the stego pixels, respectively. The constant c assures that the denominator is greater than 0. The value of contrast was calculated by Eq. (17):

$$c(\mathrm{P},\acute{\mathrm{P}}) = \frac{2 \times \delta_{\mathrm{P}} \delta_{\mathrm{P}'} + c}{\delta_{\mathrm{P}}^2 \times \delta_{\mathrm{P}}^2 + c} \tag{17}$$

In the equation (17) and equation (18), δ_{P} and $\delta_{\acute{\mathrm{P}}}$ is the standard deviations of the cover pixels and the stego pixels, respectively. The value of structural was calculated as Eq. (18):

$$S(\mathrm{P},\acute{\mathrm{P}}) = \frac{\delta_{\mathrm{PP}'} + c}{\delta_{\mathrm{P}} \delta_{\mathrm{P}'} + c} \tag{18}$$

where the covariance $\delta_{\mathrm{PP}'}$ can be calculated by Eq. (19):

$$\delta_{\mathrm{PP}'} = \frac{1}{H \times W - 1} \times \sum_{i=1}^{H} \sum_{j=1}^{W} (\mathrm{P}_{(i,j)} - \overline{\mathrm{P}})(\acute{\mathrm{P}}_{(i,j)} - \overline{\mathrm{P}}') \tag{19}$$

4.1 Performance of the proposed method

In the following images, the result and performance of the proposed method are shown.

Our proposed method, tests were performed for all 6 standard images shown in Fig. 9, and the interpretation of the

Figure 9. Test images: (a) Airplane, (b) Boat, (c) Girl, (d) Goldhill, (e) Lena, (f) Toys.

results is shown in Table 1.

According to the numerical results shown in Table 1, applying 6 standard images, the average embedding capacity is 203138 bits and the average peak signal-to-noise ratio is 51.00 dB. Also the average mean squared error and the average structural similarity index are 0.5156 and 0.9979, respectively. The average information embedding rate is 0.774 bpp, which shows that comparison of the proposed method to the previous method, especially, the competitor method in [30]. The embedding capacity and peak signal-to-noise ratio have increased significantly.

It is also necessary to reiterate that in the proposed method, using a pair of maximum and zero points of the histogram of the image prediction error, we performed the histogram shifting operation and then information embedding. In the step of image prediction error histogram shifting, the pixels that are greater than and equal to one are shifted one unit to the right in the histogram and the rest of the image prediction error pixels remain unchanged as explained in equation (1). This shift is used to detect and extract the information "1" of the embedded binary stream in the embeddable pixels of the image. This capability reduces the image distortion, unlike the method of Xie et al. [30]. As a result, for all test images and based on the results approached in Table 1, considering the high embedding rate of about 0.774 bpp, we achieved a high PSNR. Which shows the efficiency of the proposed method has been significantly increased based on the mentioned results. The comparative results of our proposed method with other three methods is analyzed in section 4.2.

Table 1. The performance of our proposed method at a glance.

Performance of the proposed scheme with 4×4 block					
Test images	EC (bit)	PSNR (db)	MSE	SSIM	ER (bpp)
Airplane	206,270	50.99	0.5176	0.9977	0.786
Boat	202,692	51.00	0.5163	0.9979	0.773
Girl	203,040	51.05	0.5105	0.9982	0.774
Goldhill	200,884	51.01	0.5149	0.9985	0.766
Lena	202,990	50.99	0.5166	0.9978	0.774
Toys	202,954	50.99	0.5177	0.9977	0.774
Average	203,138	51.00	0.5156	0.9979	0.774

4.2 Comparison of the proposed scheme with other methods

In the following, the review and comparison of the results of our method with other methods are figured out. The numerical and illustration of results are shown in Tables 2 to 4 and related figures from 10 to 13, respectively. From outcomes of our proposed scheme, embedding capacity and peak signal-to-noise ratio accompany with embedding rate have been evaluated.

As the numerical results are shown in Table 2, our proposed method is compared with the method of Xie et al. For the airplane image, compared to the competitor method, the embedding capacity increase is 25.8%, that is, we increased the capacity by 42326 bits. For the boat image, the embedding capacity increase is 48.4% that it verifies, we increased the capacity by 66141 bits. For the girl image, the embedding capacity increase is 46.7% that shows increment in the capacity by 64,691 bits. For the Goldhill image, the embedding capacity increase is 77.3%, that is, our proposed method increased the capacity by 87,641 bits. For the Lena image, the embedding capacity increase is 39.4%, this result shows the increment by 57386 bits, and finally For the toy image, the embedding capacity increase is 39.9%, that is, the proposed method increased the capacity by 57914 bits. By evaluating these results we come to conclusion that our proposed method works better in compared with the method of Xie et al. [30]. Our outcomes and approaches show a significant result compared to the method of Hu et al. [26] and Ni et al. [19].

The numerical results sorted in Table 3 show the performance of our proposed method compared with other references in term of peak signal-to-noise ratio. PSNR percentage increase for airplane image is 60.5%, for boat image is 61.8%, for girl image is 64.6%, for Goldhill image is 64.4%, for Lena's image is 62.3% and for the toy's image is 64.1%. As a result, compared to the competitor method [30], we have had a good improvement in terms of the PSNR criterion. An increase in PSNR means that the visual quality of the image is improved.

Also, the peak signal-to-noise ratio of our proposed method has been compared with the method of Hu et al. [26] and also has been compared with the method of Ni et al. [19].

Table 4, shows the comparisons between our proposed method in the criterion of embedding rate (ER) and the three related methods [19, 26, 30].

The increase of this criterion compared to the competitor's method [30] for the image of the plane and boat is 25.7% and 48.3%, respectively, for the image of the girl and the image of Goldhill, it is 46.6% and 77.3% and finally for the image of Lena and the toy, this ratio is 39.3% and 39.9%, respectively.

These results show that in criterion of information embedding rate, our proposed method has sometimes increased significantly compared to other mentioned methods.

In Fig. 10, Fig. 11, and Fig. 12 comparison of our proposed method jointly with the other 3 methods is illustrated. Regarding all standard test images are shown as a bar chart. The effectiveness and capability of our method compared to the results of previous methods; especially, the main competitor's method, has been evaluated intuitively in terms of the three criteria of EC, PSNR and ER, respectively.

In general, in the process of data and information embedding, the more information embedded in the image, the lower the quality of the image. It is because of the num-

Table 2. Comparisons among the proposed method and three related methods in terms of EC (bit) values.

Performance of the proposed method in terms of EC values						
Methods	Images					
	Airplane	Boat	Girl	Goldhill	Lena	Toys
Proposed scheme	206,270	202,692	203,040	200,884	202,990	202,954
Xie et al. [30]	163,944	136,551	138,349	113,243	145,604	145,040
Hu et al. [26]	41,329	24,938	26,255	19,905	28,785	25,979
Ni et al. [19]	9,002	5,614	3,739	2,683	2,908	9,344

Table 3. Comparisons among the proposed method and three related methods in terms of PSNR (db) values PSNR (db) values.

Performance of the proposed method in terms of PSNR values						
Methods	Images					
	Airplane	Boat	Girl	Goldhill	Lena	Toys
Proposed scheme	50.99	51.00	51.05	51.01	50.99	50.99
Xie et al. [30]	31.763	31.517	31.005	31.014	31.401	31.072
Hu et al. [26]	51.417	51.414	51.121	51.377	51.449	51.389
Ni et al. [19]	53.231	53.121	55.212	51.059	53.843	49.087

Table 4. Comparisons among the proposed method and three related methods in terms of ER (bpp) values.

Performance of the proposed method in terms of PSNR values						
Methods	Images					
	Airplane	Boat	Girl	Goldhill	Lena	Toys
Proposed scheme	0.786	0.773	0.774	0.766	0.774	0.774
Xie et al. [30]	0.625	0.5209	0.5277	0.4319	0.5554	0.5532
Hu et al. [26]	0.157	0.095	0.100	0.075	0.109	0.099
Ni et al. [19]	0.034	0.021	0.014	0.010	0.011	0.035

ber of changed pixels increases and leads the increment in image distortion. In this case, the PSNR criterion is one of the criteria for measuring image quality. In Fig. 13, our proposed method is compared with three other methods in terms of PSNR to ER ratio. The PSNR parameter has an inverse relationship with ER, generally PSNR decreases with the increase of ER. In recent years, researchers have tried to achieve a suitable PSNR by using data hiding algorithms despite the increase of ER. Fig. 13 shows the advantages of proposed method in term of the embedding rate (ER), the amount (PSNR) decreases exponentially and gradually.
For example, for a sample curve related to the airplane in Fig. 13, which is shown in blue color, the amount of PSNR in ER = 0.1967 is equal to 54.9 or in ER = 0.2623, PSNR is equal to 54.25 or in ER = 0.3934 the size of PSNR is equal to 53.18, which shows the increase of ER causes the size of PSNR is gradually decreasing. But in the method of Xie et al. [30], as shown in Fig. 13, in the image of the airplane, with the increase in the information embedding rate, the PSNR decreases steeply.
In Hu et al.'s method [26] and Ni et al.'s method [19], due to the low and limited embedding capacity, the range of changes is small compared to our proposed method. As a result, PSNR changes are in the same range.

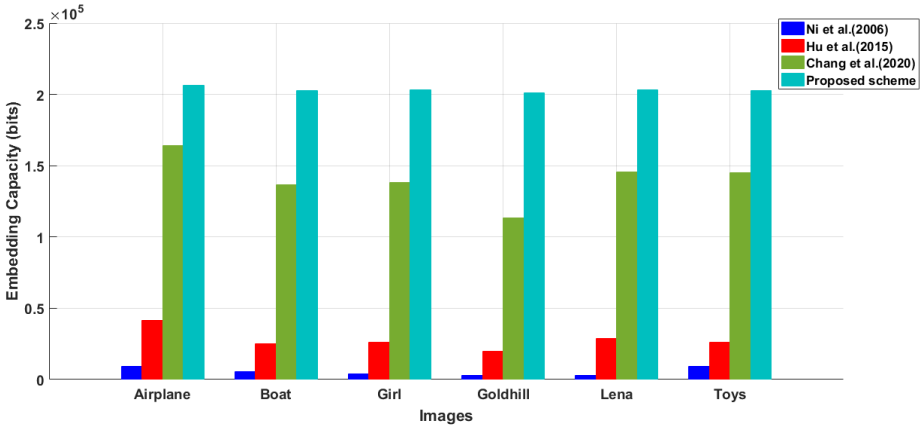

Figure 10. Comparison between the proposed method and the three related methods [19, 26, 30] in terms of EC values.

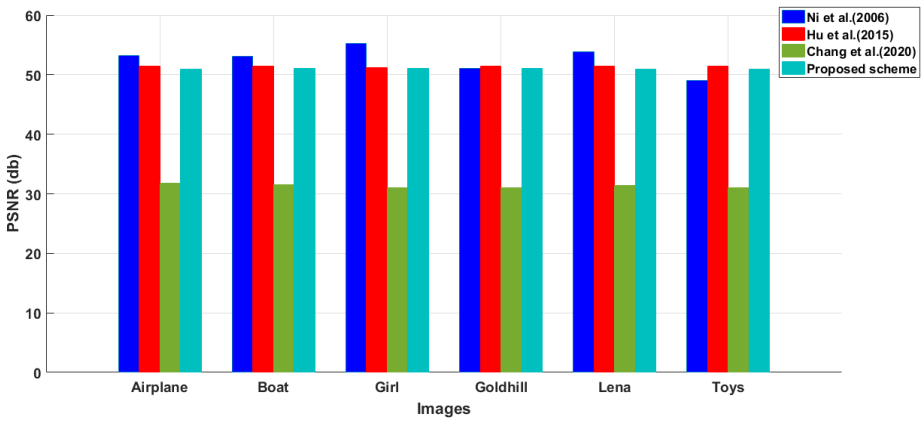

Figure 11. Comparison between the proposed method and the three related methods [19, 26, 30] in terms of PSNR values.

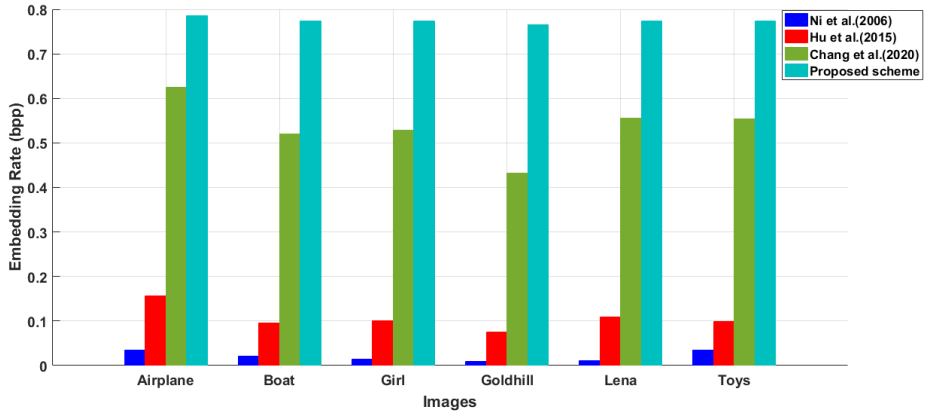

Figure 12. Comparison between the proposed method and the three related methods [19, 26, 30] in terms of ER values.

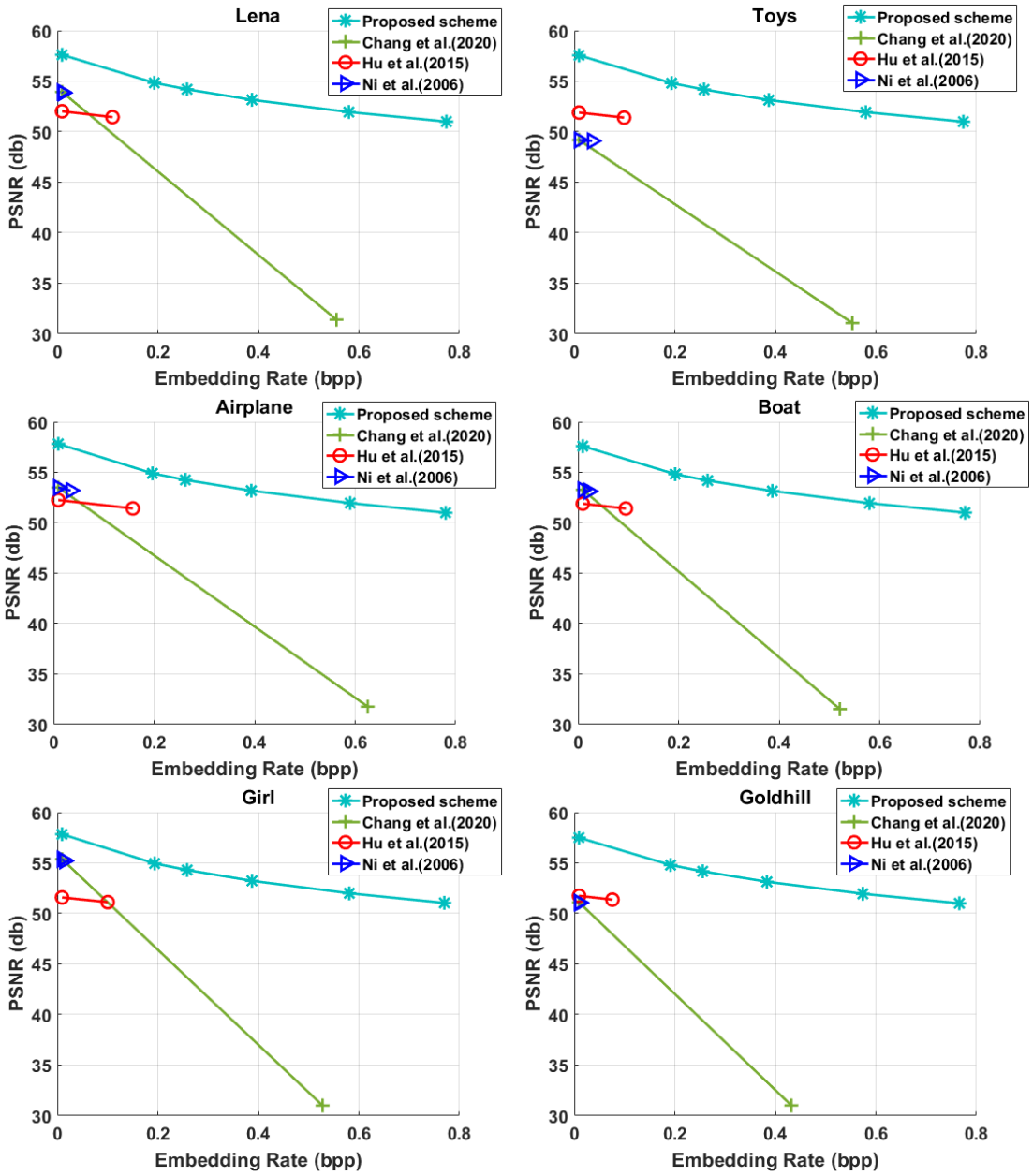

Figure 13. Comparison between the proposed method and the three related methods [19, 26, 30] in terms of embedding rates and PSNR values.

5. Conclusion

In this paper, a scheme based on histogram shifting of image prediction error with adaptive embedding capacity is proposed for reversible data hiding. The achievements of our proposed scheme show the advantages and benefits of our method in details. Using a pair of peak and zero points in the prediction- error histogram for histogram shifting operation and then information embedding to achieve high embedding capacity while maintaining image quality unlike previous methods is one of feature in our method. A block-wise based prediction is used to generate a prediction error histogram by needle shaped peak, resulting in high embedding capacity, that is also the other outcome of our method. According to the marked image, the secret data can be accurately extracted and the image can be fully recovered. Experimental results confirm that the proposed scheme can achieve higher embedding capacity than previous methods while maintaining visual quality for the marked image. In the future work, we plan to use the signed digit representation method together with the proposed method to achieve a very high embedding capacity while maintaining the image quality. Also, we are planning to apply the evolutionary and fuzzy logic algorithm in the selection and assessment of the pixels location and block- wise parts to improve our method.

Authors contributions
Authors have contributed equally in preparing and writing the manuscript.

Availability of data and materials
The data that support the findings of this study are available from the corresponding author upon reasonable request.

Conflict of interests
The authors declare that they have no known competing financial interests or personal relationships that could have appeared to influence the work reported in this paper.

References

[1] R.-Z. Wang, C.-F. Lin, and J.-C. Lin. "**Hiding data in images by optimal moderately signicant-bit replacement**.". *IEE Electron. Lett.*, 36(25):2069–2070, 2000.
DOI: https://doi.org/10.1049/el:20001429.

[2] J. Fridrich, R. Du, and M. Long. "**Steganalysis of LSB encoding in color images**.". *Proc. ICME*, 2000.
DOI: https://doi.org/10.1109/ICME.2000.871000.

[3] J. Fridrich, M. Goljan, and R. Du. "**Reliable detection of LSB steganography in grayscale and color images**.". *Proc. ACM Workshop on Multimedia and Security*, page 27–30, 2001.
DOI: https://doi.org/10.1145/1232454.1232466.

[4] J. Fridrich, M. Goljan, and R. Du. "**Invertible Authentication**.". *Proc. SPIE Security and Watermarking of Multimedia Contents*, pages 197–208, 2001.
DOI: https://doi.org/10.1117/12.435400.

[5] J. Fridrich, M. Goljan, and R. Du. "**Lossless data embedding- new paradigm in digital watermarking**.". *EURASIP J. Appl. Signal Processing*, 2002(2):185–196, 2002.
DOI: https://doi.org/10.1155/S1110865702000537.

[6] C. D. Vleeschouwer, J. F. Delaigle, and B. Macq. "**Circular Interpretation of Bijective Transformations in Lossless Watermarking for Media Asset Management**.". *IEEE Trans. Multimedia*, 5(3): 97–105, 2003.
DOI: https://doi.org/10.1109/TMM.2003.809729.

[7] C. K. Chan and L. M. Cheng. "**Hiding data in images by simple LSB substitution**.". *Pattern Recognition*, 37(3):469–74, 2004.
DOI: https://doi.org/10.1016/j.patcog.2003.08.007.

[8] H. C. Wu, N. I. Wu, C. S. Tsai, and M. S. Hwang. "**Image steganographic scheme based on pixel-value differencing and LSB replacement methods**.". *IEE Proceedings: Vision, Image & Signal Processing*, 152(5):611–5, 2005.
DOI: https://doi.org/10.1049/ip-vis:20059022.

[9] M. U. Celik, G. Sharma, A. M. Tekalp, and E. Saber. "**Unlocking Energy Efficiency: Experimental Investigation of Bamboo Fibre Reinforced Briquettes as a Sustainable Solution with Enhanced Thermal Resistance**.". *Lossless generalized-LSB data embedding*, 14(2):253–266, 2005.
DOI: https://doi.org/10.1109/TIP.2004.840686.

[10] . Zhang, X and S. Wang. "**Efficient steganographic embedding by exploiting modification direction**.". *IEEE Communication Letters*, 10(11):781–3, 2006.
DOI: https://doi.org/10.1109/LCOMM.2006.060863.

[11] M. U. Celik, G. Sharma, E. Saber, and A. M. Tekalp. "**Lossless Watermarking for Image Authentication: A new Framework and an Implementation**.". *IEEE Trans. Image Processing.*, 15(4): 1042–1049, 2006.
DOI: https://doi.org/10.1109/TIP.2005.863053.

[12] J. Tian. "**Reversible Data Embedding Using a Difference Expansion**.". *IEEE Trans. Circuits Syst. Video Technol*, 13(8):890–896, 2003.
DOI: https://doi.org/10.1109/TCSVT.2003.815962.

[13] A. M. Alattar. "**Reversible watermark using the difference expansion of a generalized integer transform**.". *IEEE Transactions on Image Processing*, 13(8):1147–56, 2004.
DOI: https://doi.org/10.1109/TIP.2004.828418.

[14] D. M. Thodi and J. J. Rodriguez. "**Expansion embedding techniques for reversible watermarking**.". *IEEE Transactions on Image Processing*, 16(3):721–30, 2007.
DOI: https://doi.org/10.1109/TIP.2006.891046.

[15] C.-C. Chang, Y.-H. Huang, H.-Y. Tsai, and C. Qin. "**Prediction-based reversible data hiding using the difference of neighboring pixels**.". *Int. J. Electron. Commun. (AEÜ)*, 66:758–766, 2012.
DOI: https://doi.org/10.1016/j.aeue.2012.01.008.

[16] C. Qin, C. C. Chang, and L. T. Liao. "**An adaptive prediction-error expansion oriented reversible data hiding scheme**.". *Pattern Recogn Lett*, 33(16):2166–2172, 2012.
DOI: https://doi.org/10.1016/j.patrec.2012.08.004.

[17] X. Qu, S. Kim, and H. J. Kim. "**Reversible watermarking based on compensation**.". *J Electr Eng Technol*, 10(1):422–428, 2015.
DOI: https://doi.org/10.5370/JEET.2015.10.1.422.

[18] C. Chang, Y. Huang, and T. Lu. "**A difference expansion based reversible data hiding scheme with high stego image visual quality**.". *Multimed Tools Appl*, 76:12659–12681, 2017.
DOI: https://doi.org/10.1007/s11042-016-3689-3.

[19] Z. Ni, Y. Q. Shi, N. Ansari, and W. Su. "**Reversible Data Hiding**.". *IEEE Transactions on Circuits and Systems for Video Technology*, 16(3):354–362, 2006.
DOI: https://doi.org/10.1109/TCSVT.2006.869964.

[20] M. Fallahpour and M. H. Sedaaghi. "**High capacity lossless data hiding based on histogram modification**.". *IEICE Electron Express*, 4(7):205–210, 2007.
DOI: https://doi.org/10.1587/elex.4.205.

[21] W. Hong, T.S. Chen, and C. W. Shiu. "**Reversible data hiding based on histogram shifting of prediction errors**.". *Proceedings of the International Symposium on Intelligent Information Technology Application Workshop*, page 292–295, 2008.
DOI: https://doi.org/10.1109/ETTandGRS.2008.263.

[22] W. Hong, T. S. Chen, and C. W. Shiu. "**Reversible data hiding for high quality images using modification of prediction errors**.". *J Syst Softw*, 82(11):1833–1842, 2009.
DOI: https://doi.org/10.1016/j.jss.2009.05.051.

[23] P. Y. Tsai, Y. C. Hu, and H. L. Yeh. "**Reversible image hiding scheme using predictive coding and histogram shifting**.". *Signal Process*, 89(6):1129–1143, 2009.
DOI: https://doi.org/10.1016/j.sigpro.2008.12.017.

[24] M. Fallahpour, D. Megias, and M. Ghanbari. "**Subjectively adapted high capacity lossless image data hiding based on prediction errors**.". *Multimedia Tools and Applications*, 2010.
DOI: https://doi.org/10.1007/s11042-010-0486-2.

[25] Z. Pan, S. Hu, X. Ma, and L. Wang. "**Reversible data hiding based on local histogram shifting with multilayer embedding**.". *J. Vis. Commun. Image Represent*, 31:64–74, 2015.
DOI: https://doi.org/10.1016/j.jvcir.2015.05.005.

[26] Y. C. Hu, P. Y. Tsai, J. S. Yeh, and W. L. Chen. "**Residual histogram shifting technique based on cascading prediction for reversible data hiding**.". *Advanced Multimedia and Ubiquitous Engineering*, page 105–110, 2015.
DOI: https://doi.org/10.1007/978-3-662-47487-7_16.

[27] W. He, G. Xiong, K. Zhou, and J. Cai. "**Reversible data hiding based on multilevel histogram modification and pixel value grouping**.". *J Vis Commun Image Represent*, 40:459–469, 2016.
DOI: https://doi.org/10.1016/j.jvcir.2016.07.014.

[28] C. Yu, X. Zhang, Z. Tang, and X. Xie. "**Separable and error-free reversible data hiding in encrypted image based on two-layer pixel errors**.". *IEEE Access*, 6:76956–76969, 2018.
DOI: https://doi.org/10.1109/ACCESS.2018.2882563.

[29] Z. Tang, S. Xu, D. Ye, J. Wang, X. Zhang, and C. Yu. "**Real-time reversible data hiding with shifting block histogram of pixel differences in encrypted image**.". *J Real-Time Image Proc*, 16(3): 709–724, 2019.
DOI: https://doi.org/10.1007/s11554-018-0838-0.

[30] X.-Z. Xie, C.-C. Chang, and Y.-C. Hu. "**An adaptive reversible data hiding scheme based on prediction error histogram shifting by exploiting signed-digit representation**.". *Multimedia Tools Appl.*, 33:34–79, 2020.
DOI: https://doi.org/10.1007/s11042-019-08402-6.

[31] L. Zhang and X. Wu. "**An edge-guided image interpolation algorithm via directional filtering and data fusion**.". *IEEE Trans. Image Process.*, 15(8):2226–2238, 2006.
DOI: https://doi.org/10.1109/TIP.2006.877407.

[32] K. H. Jung and K. Y. Yoo. "**Data hiding method using image interpolation**.". *Computer Standards and Interfaces*, 31(2):465–470, 2009.
DOI: https://doi.org/10.1016/j.csi.2008.06.001.

[33] L. Luo, Z. Chen, M. Chen, X. Zeng, and Z. Xiong. "**Reversible image watermarking using interpolation technique**.". *IEEE Trans. Inf. Forensics Secur.*, 5(1):187–193, 2010.
DOI: https://doi.org/10.1109/TIFS.2009.2035975.

[34] M. A. M. Abadi, H. Danyali, and M. S. Helfroush. "**Reversible watermarking based on interpolation error histogram shifting**.". *5th International Symposium On Telecommunications (IST)*, page 840–845, 2010.
DOI: https://doi.org/10.1109/ISTEL.2010.5734139.

[35] Y. Hanmin, Zh. Li, and L. Pu. "**Research on Reversible Date Hiding Algorithms Based on Bilinear Interpolation about Watermark**.". *3rd International Conference on E-Business, Information Management and Computer Science*, pages 592–596, 2020.
DOI: https://doi.org/10.1145/3453187.3453400.

[36] Standard Dataset Images. URL https://ccia.ugr.es/cvg/CG/base.htm.

[37] The USC-SIPI Image Database. URL https://sipi.usc.edu/database/.

[38] M. Mokhtari, M. Akhavan, and P. Derakhshan. "**Optimization of Grading Tile Using Fuzzy Image Processing and Genetic Algorithm**.". *Iranian Journal of Ceramic Science & Engineering*, 4 (3), 2015. URL http://ijcse.ir/article-1-354-en.html.